

JPET #247254

**Hepatobiliary disposition of atovaquone: A case of mechanistically unusual biliary clearance**

Mitesh Patel, Marta Johnson, Caroline J. Sychterz, Gareth J. Lewis, Cory Watson, Harma Ellens,  
Joseph W. Polli, and Maciej J. Zamek-Gliszczynski

Mechanistic Safety and Disposition, GlaxoSmithKline, King of Prussia, PA (MP, MJ, CW, HE,  
JWP, MJZ-G) and Ware, UK (GJL)

Bioanalysis, Immunogenicity, and Biomarkers, GlaxoSmithKline, King of Prussia, PA (CJS)

JPET #247254

Running Title: **Unusual biliary clearance of atovaquone**

Corresponding Author:

Maciej J. Zamek-Gliszczyński, Ph.D.

GlaxoSmithKline

709 Swedeland Rd

King of Prussia, PA 19406, USA

e-mail: maciej.x.zamek-glisczynski@gsk.com

Tel: 1-610-270-6278

Number of text pages: 34

Number of Figures: 6

Number of Tables: 3

References: 22

Abstract: 212

Introduction: 398

Discussion: 767

JPET #247254

## **Abbreviations**

AMP: Adenosine monophosphate

ATP: Adenosine triphosphate

BCRP: Breast cancer resistance protein

BSEP: Bile salt export pump

F<sub>u</sub>: Fraction unbound

K<sub>p</sub>: Ratio of liver to blood concentration

MRP2: Multidrug resistance-associated protein 2

NTCP: Sodium/taurocholate co-transporting polypeptide

OAT2: Organic anion transporter 2

OATPs: Organic anion transporting polypeptides

OCT1: Organic cation transporter 1

P-gp: P-glycoprotein

SCH: Sandwich cultured hepatocytes

JPET #247254

## Abstract

Atovaquone, an anti-protozoal and anti-pneumocystic agent, is predominantly cleared by biliary excretion of unchanged parent drug. Atovaquone is  $\geq 10,000$ -fold concentrated in human bile relative to unbound plasma. Even after correcting for apparent non-specific binding and incomplete solubility in bile, atovaquone is still concentrated 100-fold in bile, consistent with active biliary excretion. Mechanisms of atovaquone hepatobiliary disposition were studied using a multi-experimental *in vitro* and *in vivo* approach. Atovaquone uptake was not elevated in HEK293 cells singly overexpressing OATP1B1, OATP1B3, OATP2B1, OCT1, NTCP or OAT2. Hepatocyte uptake of atovaquone was not impaired by OATP and OCT inhibitor cocktail (rifamycin and imipramine). Atovaquone liver to blood ratio at distributional equilibrium was not reduced in *Oatp1a/1b* and *Oct1/2* knockout mice. Atovaquone exhibited efflux ratios of approximately unity in P-gp and BCRP overexpressing MDCK cell monolayers and did not display enhanced uptake in MRP2 vesicles. Biliary and canalicular clearance were not decreased in P-gp, Bcrp, Mrp2, and Bsep knockout rats. In the present study, we rule out the involvement of major known basolateral uptake and bile canalicular efflux transporters in the hepatic uptake and biliary excretion of atovaquone. This is the first known example of a drug cleared by biliary excretion in humans, with extensive biliary concentration, which is not transported by the mechanisms investigated herein.

JPET #247254

## Introduction

Atovaquone (Fig. 1) is an anti-protozoal active ingredient of the anti-malarial drug Malarone (atovaquone/proguanil), as well as the sole active ingredient of the pneumonia drug, Mepron (Malarone®, 2016; Mepron®, 2016). Atovaquone is predominantly cleared by biliary excretion of unchanged parent drug (Rolan et al., 1997). Metabolism is negligible with atovaquone-related metabolites not observed in plasma, feces and bile (Rolan et al., 1997; McKeage and Scott, 2003; Nixon et al., 2013). Moreover, the plasma pharmacokinetic profile of [<sup>14</sup>C]-atovaquone total radiocarbon is comparable to that observed with unlabelled parent drug, which confirms the absence of circulating metabolites. Urinary elimination is negligible, with <0.6% of the atovaquone dose recovered in the urine (Rolan et al., 1997). Collectively, these data support that biliary excretion is the major route for atovaquone elimination in humans. Notably, the concentration of atovaquone in the bile was  $\geq 10,000$ -fold higher relative to unbound plasma (Rolan et al., 1997), which suggests involvement of transporter processes in the biliary excretion of atovaquone, since passive diffusion is unlikely to produce the observed biliary concentration gradient. However, the involvement of specific transporter mechanism(s) in the biliary excretion of atovaquone has not been demonstrated to-date.

Biliary excretion is a two-step process, comprised of basolateral uptake of drugs from blood followed by canalicular excretion into the bile (Kock and Brouwer, 2012). The main objective of the present work was to elucidate transporter mechanism(s) involved in the hepatic uptake as well as canalicular efflux of atovaquone. Several hepatic uptake transporters such as organic anion transporting polypeptides (OATP1B1, OATP1B3 and OATP2B1), organic cation transporter 1 (OCT1), organic anion transporter 2 (OAT2) and sodium/taurocholate co-transporting polypeptide (NTCP) are expressed on the basolateral membrane of hepatocytes and are known to mediate

JPET #247254

uptake of substrate drugs from systemic circulation into the liver (Giacomini et al., 2010; Patel et al., 2016; Riley et al., 2016). Efflux transporters such as multidrug resistance-associated protein 2 (MRP2), breast cancer resistance protein (BCRP) and P-glycoprotein (P-gp) are expressed on the bile canalicular membrane, where they mediate drug and metabolite transport from hepatocytes into the bile. Furthermore, bile salt export pump (BSEP) transports unconjugated bile acids from liver into the bile and is sensitive to inhibition by xenobiotics; however, this transporter is not known to be a predominant mechanism for canalicular efflux of drugs. At present, the transport of atovaquone by these hepatobiliary transporters has been studied using various *in vitro* and *in vivo* models.

JPET #247254

## Materials and Methods

### Materials

[<sup>3</sup>H]-Estradiol 17 $\beta$ -D-glucuronide (specific activity 41.4 Ci/mmol), [<sup>3</sup>H]-estrone sulfate (specific activity 54 Ci/mmol), [<sup>3</sup>H]-cyclic guanosine monophosphate (specific activity 5.4 Ci/mmol), [<sup>3</sup>H]-taurocholic acid (specific activity 15.4 Ci/mmol) and [<sup>3</sup>H]-digoxin (specific activity 29.8 Ci/mmol) were purchased from Perkin Elmer (Boston, MA). [<sup>3</sup>H]-Amprenavir (specific activity 24 Ci/mmol) was purchased from GE Healthcare, (UK). [<sup>14</sup>C]-Cimetidine (specific activity 59.67 mCi/mmol) was procured from Selica Limited (Essex, UK). [<sup>14</sup>C]-Metformin hydrochloride (specific activity 110.2 mCi/mmol) was obtained from Moravsek Biochemicals, Inc. (Brea, CA). The radiochemical purity of these radiochemical compounds was  $\geq 96\%$ .

The human embryonic kidney cells (HEK-MSR2), human OATP1B1, OATP1B3 and OATP2B1 BacMam baculovirus transduction reagents were supplied by the Biological Sciences group, GlaxoSmithKline (Collegeville, PA, USA). Human embryonic kidney cells transiently overexpressing OCT1, OAT2 or NTCP and control cells were purchased from Corning® (New York, USA). Cryopreserved pooled human hepatocytes for uptake studies and in Vitro CP media were purchased from Celsis (Baltimore, MD). Madin-Darby Canine Kidney Epithelial (MDCK) cells overexpressing MDR1 (MDCK-MDR1) and BCRP (MDCK-BCRP) were obtained from the Netherlands Cancer Institute. MRP2, control vesicles and transport assay kits were purchased from Genomembrane (Yokohama, Japan). Rat SCH plates were purchased from Qualyst Transporter Solution, LLC (QTS, Durham, NC). QTS Transporter certified<sup>TM</sup> human hepatocytes for biliary excretion studies were purchased from Triangle Research Laboratories (TRL, Research Triangle Park, NC). B-CLEAR® assay reagents were purchased from QTS (Durham, NC).

JPET #247254

Atovaquone, taurocholic acid, Lucifer yellow, digoxin, indomethacin, cyclosporine, cyclic guanosine monophosphate and imipramine were procured from Sigma-Aldrich (St. Louis, MO). GF120918, atovaquone-d4 and unlabelled APV were supplied by Santa Cruz Biotechnology (Dallas, TX). Rifamycin SV was purchased from Toronto Research Company (Toronto, Canada). Montelukast was purchased from Cayman Chemical Company (Ann Arbor, MI). Matrigel® (9.3 mg/mL), collagen and poly-D-lysine coated 24-well plates were obtained from Corning (Tewksbury, MA). Transwell® inserts for P-gp and BCRP assays were obtained from BD Biosciences (Bedford MA) and Greiner Bio-One (Frickenhausen, Germany), respectively. Teflon 96-well dialysis block and 1 kDa dialysis membranes were purchased from HTDialysis (Gales Ferry, CT).

## **Methods**

### **Apparent Biliary Binding and Solubility**

Equilibrium dialysis of rat bile spiked with 1  $\mu$ M atovaquone against buffer was conducted to determine the apparent fraction unbound as described previously (Zamek-Gliszczynski et al., 2011) with the following modifications: dialysis membrane pore size was 1 kDa and dialysis was carried out for 24 hours. In addition, plasma spiked with 1  $\mu$ M atovaquone was dialyzed against bile in the same manner.

Rat bile was spiked with 30  $\mu$ g/mL atovaquone, vortex mixed, and centrifuged at 15,000g for 10 minutes. Initial (uncentrifuged), and post-centrifugation concentrations were determined at the top, middle, and bottom of the centrifuge tube.

## **Cell Culture**

### **OATPs**

JPET #247254

HEK-MSR2 cells were transduced with OATP-BacMam (OATP1B1, OATP1B3 or OATP2B1) or null virus in DMEM Ham's F-12 media containing 10% FBS, 0.4 mg/mL geneticin and 2 mM sodium butyrate. Briefly, cells were thawed and immediately transferred to DMEM Ham's F-12 medium. Following centrifugation at 1,500 rpm for 5 min, media was aspirated and cells were resuspended in fresh medium. A small aliquot was collected for cell counting as well as viability assessment by Trypan Blue exclusion method. Cells were seeded at a density of  $0.4 \times 10^6$  cells/well in poly-D-lysine coated 24-well plates and maintained at 37°C, 5% CO<sub>2</sub>, and 95% humidity for 48 h.

### **OCT1, OAT2 and NTCP**

Cells were rapidly thawed and transferred to pre-warmed DMEM with 10% FBS and MEM non-essential amino acids. Cells were centrifuged at 100 g for 10 min. Media was aspirated and the cell pellet was resuspended in fresh medium. Following viability assessments, cells were seeded at a density of  $0.4 \times 10^6$  cells/well and maintained at 37°C with 5% CO<sub>2</sub> and minimal humidity for 4 h. Media was replaced and cells were incubated overnight at 37°C with 5% CO<sub>2</sub> and minimal humidity.

### **Human hepatocytes**

Cryopreserved human hepatocytes were thawed and immediately resuspended in *InVitroGRO* plating media. An aliquot was removed for cell counting as well as viability assessment. Cells were seeded at a density of  $0.375 \times 10^6$  cells/well in collagen coated 24-well plates. Hepatocytes were incubated at 37°C with 5% CO<sub>2</sub> for approximately 5 h prior to the initiation of the uptake study.

### **P-gp and BCRP**

JPET #247254

Cells were thawed and suspended in DMEM supplied with glutamax, 10% FBS, 50 U/mL penicillin and 50 µg/mL streptomycin. Following centrifugation at 4000 rpm for 5 min, media was aspirated and cells were resuspended in DMEM. MDCK-MDR1 cells were diluted to obtain a final concentration of 280,000 cells/mL and 450 µL of cell suspension was added to the Transwell® inserts whereas, the basolateral chamber was filled with 1.3 mL of DMEM. MDCK-BCRP cells were seeded at a density of 200,000 cells/cm<sup>2</sup> in Transwell® inserts and the basolateral chamber contained 1.2 mL of DMEM. Cells were incubated overnight at 37°C, 5% CO<sub>2</sub> and 95% humidity. The following day, media was replaced and cells were maintained at 37°C, 5% CO<sub>2</sub> and 95% humidity before initiation of the transport study.

### **Human SCH**

Hepatocytes were thawed and immediately transferred to cryopreserved hepatocyte thawing media. Following centrifugation at 100 g for 8 min, cells were resuspended and seeded at a density of 0.4 x 10<sup>6</sup> cells/well in collagen coated 24-well plates. Cells were incubated at 37°C, 5% CO<sub>2</sub> and 95% humidity for 4 h. Media was replaced and cells were incubated for 24 h. Following day, cells were overlaid with Matrigel® (0.3 mg/mL) and maintained in cell culture media for 96 h prior to initiation of biliary excretion studies.

### **Cellular uptake studies**

The substrate potential of atovaquone was determined with uptake studies in singly expressing OATP1B1, OATP1B3, OATP2B1, OCT1, OAT2 or NTCP relative to control HEK293 cells in the presence and absence of prototypical inhibitors. Briefly, cell monolayer was washed two times with transport medium and pre-incubated with transport media containing a transporter inhibitor or DMSO at 37°C for 20 min. Pre-incubation solution was aspirated and 400 µL of atovaquone

JPET #247254

solution with and without an inhibitor was added and incubated at 37°C. The solution was removed and cells were rapidly rinsed three times with 400 µL cold transport media. About 200 µL of distilled deionized water was added to each well and plates were stored overnight at -20°C for cell lysis.

Simultaneously, [<sup>3</sup>H]-estradiol 17β-D-glucuronide uptake was carried out in HEK-OATP1B1 and HEK-OATP1B3 cells in the presence and absence of rifamycin to demonstrate the functionality of these transporters. [<sup>3</sup>H]-Estrone sulfate uptake was carried out in the presence and absence of montelukast in HEK-293 cells overexpressing OATP2B1. Cells were lysed with 0.1% (v/v) Triton X-100 in phosphate-buffered saline. An aliquot was suspended in 5 mL scintillation fluid and analyzed with liquid scintillation spectroscopy.

The cellular uptake study of positive controls and atovaquone was carried out in HEK-OCT1, HEK-OAT2 and HEK-NTCP cells in the presence and absence of a prototypical inhibitor without any preincubation. The uptake study in these cells was carried out according to the protocol as described above. The uptake of [<sup>14</sup>C]-metformin was carried out in the presence or absence of imipramine in HEK-OCT1 cells to examine the functional activity of the test system. For HEK-OAT2 and HEK-NTCP cells, [<sup>3</sup>H]-cyclic guanosine monophosphate and [<sup>3</sup>H]-taurocholic acid uptake was carried out in the absence and presence of indomethacin and cyclosporine, respectively.

An uptake of [<sup>3</sup>H]-estradiol 17β-D-glucuronide and atovaquone was also studied in cryopreserved pooled plated human hepatocytes in the absence and presence of an OATP and OCT inhibitor cocktail (rifamycin and imipramine, 100 µM each).

### **Transepithelial bidirectional transport studies**

JPET #247254

Following 96 h incubation, DMEM was carefully aspirated from the apical and basolateral chambers without disturbing the cell monolayer. MDCK-MDR1 and MDCK-BCRP cells were pre-incubated in DMEM (without phenol red or serum) with and without GF120918 at 37°C and 70 rpm for 20 min. To determine apical to basolateral transport, atovaquone solution was added to the apical chamber and the basolateral chamber contained fresh transport media. To determine basolateral to apical transport, atovaquone solution was added to the basolateral chamber and the apical chamber was filled with fresh transport media. Plates were incubated at 37°C and 70 rpm for 90 min. Following incubation, samples were collected from apical as well as basolateral chambers and stored at -70°C or lower until analysis.

Simultaneously, [<sup>3</sup>H]-amprenavir and [<sup>14</sup>C]-cimetidine transport was studied to determine the functional activity of P-gp and BCRP in MDCK-MDR1 and MDCK-BCRP cells, respectively. The transport of positive controls and atovaquone across MDCK-MDR1 and MDCK-BCRP cells was also studied in the presence of GF120918 (P-gp and BCRP inhibitor), respectively.

### **MRP2 vesicular transport studies**

The transport of atovaquone was studied in commercially available inside-out MRP2 vesicles according to a protocol recommended by Genomembrane. Briefly, vesicles were preincubated with bromosulphophthalein, a MRP2 inhibitor or DMSO at 37°C for 10 min and then incubated with atovaquone in 50 mM MOPS-Tris buffer (pH 7.0) containing adenosine triphosphate (ATP) or adenosine monophosphate (AMP) at 37°C for 10 min. Following incubation, the transport process was terminated with 200 µL of ice-cold stop solution (400 mM MOPS-Tris, 700 mM KCl). The reaction mixture was immediately transferred to a glass filter plate (Millipore, MultiScreen®<sub>HTS</sub> FB Filter Plate) and quickly washed three times with 200 µL of ice-cold stop solution. The filter

JPET #247254

was carefully removed from each well and placed in eppendroff tubes containing 100  $\mu$ L of acetonitrile:distilled deionized water (1:1). Tubes were stored at -20°C until further analysis.

Simultaneously, the uptake of [ $^3$ H]-estradiol 17 $\beta$ -D-glucuronide was studied to investigate the functionality of MRP2 vesicles. To determine [ $^3$ H]-estradiol 17 $\beta$ -D-glucuronide concentrations, the filter plate was dried at 50°C for about 30 min and 100  $\mu$ L of microscint fluid was added to each well. The plate was covered with a TopSeal clear adhesive film and the radioactivity was measured with a TopCount® NXT HTS detector (Perkin Elmer, Waltham, MA).

### ***In vivo* pharmacokinetics**

All animal procedures were IACUC approved and conducted in compliance with the Animal Welfare Act Regulations (9 CFR Parts 1, 2 and 3) and the ‘Guide for the Care and Use of Laboratory Animals’ (ILAR, 1996) as well as all GSK company policies and guidelines.

### **Intravenous (IV) pharmacokinetic studies**

Oatp1a/1b knockout, Oct1/2 knockout and wild-type FVB mice (n=4 per group), weighing about 30 g, were purchased from Taconic Inc. (New Jersey, US). Animals were housed in individually plastic containers in a controlled environment and were provided with free access to appropriate diet and water for the entire duration of the study. A 0.2 mg/mL atovaquone solution was formulated in 5% DMSO and 20% Captisol in saline, pH 9 and filtered through 0.2  $\mu$ m sterile filters. Animals were administered with an IV bolus dose of atovaquone, as a slow bolus push, at a target dose of 1 mg/kg. At predetermined time points (0.17, 1, 2, 4, 6, 24, 28, 30 h), 25  $\mu$ L of blood samples were collected in EDTA-coated capillary tubes, mixed with an equal volume of water and stored at -70°C until analysis. After the last blood sample was collected, mice were

JPET #247254

euthanized by carbon dioxide asphyxiation followed by exsanguinations. Livers were extracted, rinsed with ice-cold saline, blotted dry and stored at -70°C until homogenization in distilled deionized water. The weight of livers and resulting homogenates were determined.

### **Continuous infusion studies**

Mdr1a/b (P-gp) knockout, Bcrp knockout, Mrp2 knockout, Bsep knockout and wild-type male Sprague-Dawley rats (n = 6) were purchased from SAGE Horizon Discovery Group (Boyertown, PA). Rats were surgically cannulated in the bile duct and femoral vein. Rats were allowed at least a 72 h post-surgical recovery period prior to use in the study. Animals were kept in individual plastic metabolism cages due to their surgical status (i.e. cannulation) and set-up to allow continuous atovaquone and bile salt infusion and collection. Animals were provided with certified food and tap water ad libitum for the entire duration of the study. Atovaquone solution, 0.5 and 0.05 mg/mL, was prepared in 5% dimethyl sulfoxide (DMSO) and 20% captisol in saline and filtered through 0.2 µm sterile filter. The bile salt replacement solution (sodium taurocholate, 2 mg/mL) was prepared in saline and sterile filtered through a 0.2 µm filter. Bile salts were infused at a rate of 15 µL/min.

Rats were given a single IV loading dose of 2.5 mg/kg, as a slow bolus push via the femoral vein catheter, and immediately followed with a continuous infusion at 0.1 mg/kg/h for 30 h. Blood samples (25 µL) were collected at predetermined time points (0.17, 1, 2, 4, 6, 24, 28, 30 h) after infusion was initiated via tail snip and transferred into labeled tubes containing an equal volume of water (1:1). Bile was collected over the same time interval and the weight was determined. Blood and bile samples were stored at -70°C until analysis. After 30 h blood and bile sample collection, infusion was stopped and rats were euthanized to collect the liver. Livers were rinsed with ice-cold saline, blotted dry and stored at -70°C or lower until homogenization with water

JPET #247254

using a GentleMACs homogenizer. All samples were stored at approximately -70°C or lower until further analysis.

### **Sandwich cultured hepatocyte studies**

Biliary excretion studies of positive controls and atovaquone in rat and human SCH were conducted post 72 and 96 h overlay with Matrigel®, respectively. Briefly, SCH were washed with 0.5 mL Ca<sup>2+</sup> containing or Ca<sup>2+</sup>-free buffer twice and incubated with the same buffer at 37°C for 10 min to conserve or disrupt bile canalicular tight junctions. Buffers were removed and cells were incubated with atovaquone solution at 37°C for 10 min. Following incubation, cells were rinsed three times with 0.5 mL ice-cold standard buffer. Cells were lysed in 200 uL distilled deionized water at -20°C and samples were analyzed using ultra high-performance liquid chromatography-tandem mass spectrometry (UPLC-MS/MS).

Simultaneously, uptake of probe substrates such as [<sup>3</sup>H]-digoxin (P-gp), [<sup>3</sup>H]-taurocholic acid (BSEP) and [<sup>3</sup>H]-estradiol 17β-D-glucuronide (MRP2) in SCH exposed to Ca<sup>2+</sup> containing or Ca<sup>2+</sup>-free buffer was carried out to test the functionality of the system. Cells were lysed with 0.1% (v/v) Triton X-100 in phosphate-buffered saline. Samples were suspended in 5 mL scintillation fluid and analyzed by liquid scintillation spectroscopy.

The cellular uptake in rat SCH was normalized with protein concentration quantified with BCA protein assay (Thermo Scientific, Rockford, IL) by using bovine serum albumin as a reference standard. Whereas, the cellular uptake in human SCH was normalized with seeding density which was 0.4 x 10<sup>6</sup> million cells/well.

### **Sample Preparation**

JPET #247254

Atovaquone samples were extracted using liquid-liquid extraction and analyzed with UPLC-MS/MS. Briefly, Artic White 96-well polypropylene extraction plate was washed with 1 mL of *tert*-Butyl methyl ether and dried under a steady stream of nitrogen gas heated to 45°C. Atovaquone-d4 (IS) in acetonitrile:water (1:1) was mixed with 50 µL of atovaquone samples in the extraction plate and vortexed for 1 min. Analytes were extracted with 1 mL of *tert*-butyl methyl ether for 4 min. The plate was centrifuged at 4000 rpm for 5 min and about 900 µL of the organic solvent was carefully collected. The organic solvent was evaporated and samples were reconstituted in 100 µL of acetonitrile:water (1:1) for UPLC-MS/MS analysis.

UPLC was performed using a Waters Acquity UPLC® system (Milford, MA). Chromatographic separation was achieved with a gradient of 0.1% formic acid in water and acetonitrile on a Acquity BEH C18, 2.1 mm x 50 mm, 1.7 µ column (Milford, MA) maintained at 65°C. The mobile phase was pumped at 0.75 mL/min and chromatographs were obtained for 2 min. Atovaquone and IS eluted at 1.25 and 1.24 min, respectively. Samples were analyzed by negative ion turbo ionspray MS/MS with an Applied Biosystems/MDS Sciex API 4000™ (Ontario, Canada). MRM transition (m/z) for atovaquone and IS was 365/337.2 and 371.2/343.2, respectively. MS/MS was conducted using nitrogen as collision gas. Operational parameters such as declustering potential (DP): -110 V; collision energy (CE): -42 V; entrance potential (EP) -10 V; and collision cell exit potential (CXP) -9 V were also optimized. The ion spray and collision gas pressure parameters were also optimized (ion spray voltage: -4500 V, temperature: 650 °C, collision gas: 12 psi, curtain gas: 20 psi). Raw data was integrated using Applied Biosystems/MDS Sciex software Analyst v 1.6.1 (Ontario, Canada). The peak area (analyte/IS) ratios was calculated to construct calibration curves from which the concentrations of atovaquone in the samples were determined.

## Data Analysis

JPET #247254

## Transepithelial bidirectional transport studies

The rate of transport (nmol/cm<sup>2</sup>/h) was calculated with Eq. 1.

$$\text{Rate of transport} = \left( \frac{\text{total nmol transported}}{T \times A} \right) \quad (1)$$

Where T and A are time (h) and surface area (cm<sup>2</sup>).

Efflux ratio was determined in the absence and presence of the Pgp and BCRP inhibitor, GF120918 using Eq. 2.

$$\text{Efflux ratio} = \left( \frac{\text{Drug transport B} \rightarrow \text{A}}{\text{Drug transport A} \rightarrow \text{B}} \right) \quad (2)$$

The permeability coefficient (P) of Lucifer Yellow at pH 7.4 was determined using Eq. 3

$$P = - \left( \frac{V_D V_R}{(V_D + V_R) A t} \right) \text{Ln} \left\{ 1 - \frac{(V_D + V_R) C_R}{(V_D C_D + V_R C_R)} \right\} \times 10^7 \quad (3)$$

Where, V<sub>D</sub> and V<sub>R</sub> are donor and receiver well volumes (mL), respectively. C<sub>R</sub>(t) and C<sub>D</sub>(t) are the concentration (nmol/mL) in the receiver and donor well at time t (90 min). Only cell monolayers with permeability rates of ≤ 50 nm/s for Lucifer yellow were used in determining permeability rates of positive controls and atovaquone.

## Biliary and canalicular clearance

Biliary excretion index (%), *in vitro* biliary and canalicular clearances were calculated as previously described (Nakakariya et al., 2012). Biliary excretion index (%) was calculated by using Eq. 4.

$$\text{Biliary excretion index (\%)} = \left( \frac{\text{Accumulation}_{(\text{cells} + \text{bile})} - \text{Accumulation}_{(\text{cells})}}{\text{Accumulation}_{(\text{cells} + \text{bile})}} \right) \times 100 \quad (4)$$

JPET #247254

Where Accumulation<sub>(cells + bile)</sub> and Accumulation<sub>(cells)</sub> represents accumulation of positive controls or atovaquone in SCH pre-exposed to Ca<sup>2+</sup> or Ca<sup>2+</sup>-free buffer, respectively.

*In vitro* biliary clearance in rat SCH was determined using Eq. 5

$$\text{In vitro biliary clearance} = \left( \frac{\text{Accumulation}_{(\text{cells} + \text{bile})} - \text{Accumulation}_{(\text{cells})}}{\text{AUC}_{\text{medium}}} \right) \quad (5)$$

Where AUC<sub>medium</sub> represents a product of incubation time and nominal media concentration of atovaquone. *In vitro* biliary clearance values were scaled from mL/min/mg protein to mL/min/kg body weight by using 200 mg protein per g liver weight and 40 g liver per kg body weight (Nakakariya et al., 2012). *In vivo* biliary clearance was predicted using well stirred models and are presented as Eq. 6 and Eq. 7.

$$\text{Predicted in vivo biliary clearance} = \left( \frac{Q_H \times \text{in vitro CL}_{\text{biliary}}}{Q_H + \text{in vitro CL}_{\text{biliary}}} \right) \quad (6)$$

Where Q<sub>H</sub> represents hepatic blood flow and is 55.2 mL/min/kg body weight (Davies and Morris, 1993). However, if fraction unbound (f<sub>u</sub>), which is 0.001 for atovaquone (Mepron®, 2016), is considered, then Eq. 6 is modified to Eq. 7 as presented below

$$\text{Predicted in vivo biliary clearance} = \left( \frac{Q_H \times f_u \times \text{in vitro CL}_{\text{biliary}}}{Q_H + f_u \times \text{in vitro CL}_{\text{biliary}}} \right) \quad (7)$$

Canalicular clearance of atovaquone in rat SCH was determined based on hepatocyte concentration as shown in Eq. 8 and 9.

$$\text{In vitro canalicular clearance} = \left( \frac{\text{Accumulation}_{(\text{cells} + \text{bile})} - \text{Accumulation}_{(\text{cells})}}{\text{Incubation time} \times \text{hepatocyte concentration}} \right) \quad (8)$$

Hepatocyte concentration was calculated by using Eq. 9

$$\text{Hepatocyte concentration} = \left( \frac{\text{Accumulation}_{(\text{cells})}}{\text{Intracellular space}} \right) \quad (9)$$

JPET #247254

Where, intracellular space used was 5.2  $\mu\text{L}/\text{mg}$  protein.

For human SCH, *in vitro* biliary clearance was calculated using Eq. 5 and was further scaled from mL/min/million cells to mL/min/kg assuming  $120 \times 10^6$  hepatocytes per g liver weight and 25.7 g liver per kg body weight (Bayliss et al., 1999; Kotani et al., 2011). *In vivo* biliary clearance was predicted with Eq. 6 and 7 using hepatic blood flow as 20.7 mL/min/kg body weight (Davies and Morris, 1993).

*In vivo* biliary clearance was determined from cumulative amount of atovaquone accumulated in bile over 30 h and area under the blood concentration-time curve ( $\text{AUC}_{0-30\text{h}}$ ) of atovaquone as shown in Eq. 10.

$$\text{In vivo biliary clearance} = \left( \frac{\text{Cumulative amount accumulated in bile}}{\text{AUC}_{0-30\text{h}}} \right) \quad (10)$$

*In vivo* canalicular clearance was determined based on liver concentrations of atovaquone as shown in Eq. 11.

$$\text{In vivo canalicular clearance} = \left( \frac{\text{Steady state biliary excretion rate}}{\text{Liver concentration at 30 h}} \right) \quad (11)$$

The *in vitro* and *in vivo* canalicular clearance were compared considering  $f_u$  is equal in SCH and liver. Therefore, canalicular clearance was calculated based on total atovaquone concentrations in hepatocytes and liver.

### Pharmacokinetic analysis

Pharmacokinetic analysis of atovaquone blood concentration-time data was performed by a non-compartmental method using Phoenix WinNonlin™, Version 6.3. All computations utilized

JPET #247254

nominal sampling times and actual doses recorded during the study. The AUC from the time of dosing to the last quantifiable time point ( $AUC_{0-t}$ ) was determined using the linear up-logarithmic down trapezoidal rule.

### **Statistical analysis**

Student's *t*-test with Bonferroni's correction for multiple comparisons was employed to determine statistical significance with correction for unequal variance, where applicable as determined by the *f*-test. In all cases,  $p < 0.05$  was considered statistically significant.

JPET #247254

## Results

### Apparent Biliary Binding and Solubility

Bile apparent fraction unbound was  $14.3 \pm 8.7\%$ . Dialysis of plasma against bile yielded an apparent equilibrium bile/plasma ratio of  $0.008 \pm 0.004$ . As expected, based on theoretical principles, the apparent bile/plasma ratio is in good agreement with the fraction unbound ratio of bile/plasma (Di et al., 2017).

Following centrifugation of bile spiked with 30  $\mu\text{g/mL}$  atovaquone, concentration at top and middle of tube was  $11.4 \pm 3.3\%$  and  $10.1 \pm 1.8\%$  of starting concentration. Atovaquone at the bottom of the tube were approximately 2.6-fold higher than starting concentration and 22.9-fold higher than the concentration at the top of the tube following centrifugation.

### Cellular uptake

The cellular uptake of positive controls and atovaquone was studied in singly expressing and control HEK293 cells (Fig. 2). The uptake of [ $^3\text{H}$ ]-estradiol 17 $\beta$ -D-glucuronide, a positive control of OATP1B1, was significantly higher in OATP1B1 overexpressing relative to control HEK cells and reduced significantly in the presence of rifamycin demonstrating functional expression of OATP1B1. In contrast, the uptake of atovaquone in HEK-OATP1B1 cells was comparable relative to control HEK cells and was not diminished in the presence of rifamycin. Similarly, atovaquone uptake was not enhanced in OATP1B3, OATP2B1, OCT1, OAT2 or NTCP overexpressing cells relative to control HEK293 cells and was comparable in the presence of prototypical inhibitors of these transporters. Functional expression of all 6 uptake transporters studied was confirmed with markedly enhanced uptake of a prototypical substrate (vs. control cells), which was significantly reduced by co-incubation with a prototypical inhibitor.

JPET #247254

An uptake study was also carried out in human hepatocytes in the absence and presence of an uptake inhibitor cocktail (rifamycin and imipramine, 100  $\mu$ M each). Atovaquone uptake clearance in human hepatocytes was not impaired in the presence of the inhibitor cocktail, whereas the uptake clearance of positive control estradiol 17 $\beta$ -D-glucuronide was significantly inhibited (Fig. 3).

### **Oatp1a/1b and Oct1/2 knockout studies**

Blood concentrations versus time profiles of atovaquone in Oatp1a/1b knockout, Oct1/2 knockout and wild-type mice following IV bolus administration are presented in Fig. 4. Pharmacokinetic parameters are summarized in Table 1. Following a single IV bolus dose, systemic exposure of atovaquone was not significantly increased in Oatp1a/1b and Oct1/2 knockout relative to wild-type mice. Moreover, atovaquone liver-to-blood concentration ratio at distributional equilibrium in Oatp1a/1b- and Oct1/2-knockout mice was not decreased, as would be expected for a compound taken up into the liver by these knocked out transporters.

### **P-gp and BCRP monolayer flux**

The permeability of Lucifer yellow in MDCK-MDR1 and MDCK-BCRP cell monolayers in the apical-to-basolateral as well as basolateral-to-apical directions was lower than 50 nm/s, which is a pre-determined cut-off value established in our laboratory for monolayer integrity. The efflux ratio of positive controls across MDCK-MDR1 and MDCK-BCRP monolayers was found to be  $\geq 4$  and reduced to unity in the presence of GF120918, a potent P-gp and BCRP inhibitor, demonstrating functional expression of P-gp and BCRP, respectively.

The efflux ratio of atovaquone in MDCK-MDR1 and MDCK-BCRP monolayers was approximately unity and remained unaltered in the presence of GF120198 (Fig. 5).

JPET #247254

## **MRP2 vesicular transport studies**

[<sup>3</sup>H]-Estradiol 17 $\beta$ -D-glucuronide vesicular uptake was approximately 30-fold stimulated in the presence of ATP and diminished significantly by bromosulphophthalein, demonstrating functional expression of MRP2. In contrast, the uptake of atovaquone in AMP- and ATP-treated vesicles was comparable, and it remained unaltered in the presence of bromosulphophthalein in ATP-treated MRP2 vesicles (Fig. 5).

## **P-gp, Bcrp, Mrp2 and Bsep knockout studies**

To determine the role of Bcrp, P-gp, Mrp2, and Bsep in the biliary excretion of atovaquone, steady-state biliary and canalicular clearances were determined in relevant transporter knockout and wild-type rats. The unbound blood and bile concentration versus time profiles of atovaquone in wild-type rats are depicted in Fig. 6. In this infusion protocol, atovaquone concentration in blood and biliary excretion rate reached a plateau within 4 h. Similarly, atovaquone steady-state was achieved by 4 h in transporter knockout rats (figures not shown). Blood AUC<sub>0-30h</sub>, biliary recovery, steady-state biliary excretion rate and liver K<sub>p</sub> of atovaquone was comparable in transporter knockout and wild-type rats (Table 2). The biliary and canalicular clearance of atovaquone in Bcrp, P-gp, Mrp2 and Bsep knockout rats was not diminished relative to wild-type rats (Table 2). Moreover, systemic AUC as well as liver K<sub>p</sub> of atovaquone were not increased in knockout rats, as would be expected for a compound excreted in bile by these knocked out transporters.

## **Biliary Clearance in rat SCH**

Accumulation of positive controls in rat SCH was assessed to examine the functionality of the cell system. [<sup>3</sup>H]-taurocholate, [<sup>3</sup>H]-digoxin and [<sup>3</sup>H]-estradiol 17 $\beta$ -D-glucuronide were selected as positive controls since these compounds are substrates of bile canalicular transporters BSEP, P-

JPET #247254

gp, and MRP2, respectively (Wolf et al., 2008). Biliary excretion index values obtained for [ $^3$ H]-taurocholate, [ $^3$ H]-digoxin and [ $^3$ H]-estradiol 17 $\beta$ -D-glucuronide were  $60 \pm 1\%$ ,  $34 \pm 8\%$  and  $10 \pm 8\%$ , respectively, which is in the accepted range for hepatocytes with functionally active bile canalicular efflux transporters (Wolf et al., 2008; Mohamed and Kaddoumi, 2013).

The *in vitro* biliary clearance of atovaquone was  $5 \pm 5$   $\mu$ L/min/mg protein (Eq. 5). Predicted *in vivo* biliary, with and without correction for plasma protein binding, and canalicular clearances for atovaquone are presented in Table 3. An IVIVE for biliary and canalicular clearances of atovaquone was attempted based on the *in vitro* and *in vivo* data obtained from the present studies (Table 2 and 3). The biliary clearance was over predicted by about 630-fold with well-stirred model not corrected for plasma protein binding, but the prediction was accurate when corrected for plasma protein binding. *In vitro* canalicular clearance determined using total hepatocyte concentration over predicted *in vivo* clearance by approximately 11-fold.

### **Biliary Clearance in human SCH**

The transport of positive controls was carried out in human SCH to examine the functionality of the test system. Biliary excretion index of [ $^3$ H]-taurocholate and [ $^3$ H]-digoxin was  $67 \pm 7\%$  and  $51 \pm 2\%$ , respectively. The *in vitro* biliary clearance of atovaquone was found to be  $1 \pm 1$   $\mu$ L/min/million cells (Eq. 5). Predicted *in vivo* biliary clearance for atovaquone obtained using well stirred model with and without correction for plasma protein binding is presented in Table 3. An IVIVE for biliary clearance of atovaquone was attempted using the data obtained from human SCH. The biliary clearance of atovaquone in humans was estimated to be 0.15 mL/min/kg (Rolan et al., 1997). Based on these data, the biliary clearance was over predicted by 15-fold with well-stirred model not corrected for plasma protein binding (Eq. 6), but under predicted by approximately 50-fold when corrected for plasma protein binding (Eq. 7).

JPET #247254

## Discussion

Atovaquone, an anti-protozoal and anti-parasitic agent, is indicated in the treatment of malaria and pneumocystis carinii pneumonia. Atovaquone is predominantly cleared by biliary excretion of parent drug with biliary concentrations  $\geq 10,000$ -fold higher than unbound plasma concentrations (Rolan et al., 1997), which suggests involvement of transporters in the excretion of atovaquone in the bile. Even after correcting for approximately one order of magnitude apparent non-specific binding and another one order of magnitude incomplete solubility in bile, atovaquone is still concentrated 100-fold in bile relative to unbound plasma, consistent with active biliary excretion. In the present work, a multi-experimental approach was used to investigate atovaquone transport by major hepatobiliary transporters.

Atovaquone uptake was not enhanced in OATP1B1, OATP1B3, OATP2B1, OCT1, OAT2 or NTCP overexpressing cells relative to control HEK293 cells and was not decreased in the presence of prototypical inhibitors of these transporters. Likewise, atovaquone uptake was not affected by an uptake inhibitor cocktail in human hepatocytes. Finally, Oatp1a/1b and Oct1/2 knockout mice were used to confirm *in vivo* relevance of the negative findings from the uptake studies in transporter overexpressing HEK293 cells and human hepatocytes. Although a positive control substrate was not included in the animal studies, large decreases in liver  $K_p$  and increases in systemic exposure of statins and metformin have been previously reported in Oatp1a/1b- and Oct1/2-knockout mice, respectively (Higgins et al., 2014). However, liver  $K_p$  of atovaquone was comparable in Oatp1a/1b knockout, Oct1/2 knockout and wild-type mice. Collectively, these data suggest that atovaquone is not taken up into the liver by OATP1B1, OATP1B3, OATP2B1, OCT1, OAT2 and NTCP.

JPET #247254

Transport of atovaquone by bile canalicular transporters such as BCRP, P-gp, MRP2 and BSEP was determined since these transporters have been widely known to play an important role in the transport of xenobiotics and endogenous compounds from liver into the bile (Patel et al., 2016). The transport of atovaquone across MDCK-MDR1 and MDCK-BCRP cells yielded an efflux ratio of approximately unity and remained unchanged in the presence of GF120918. Moreover, atovaquone transport in ATP- and AMP-treated MRP2 vesicles was comparable and was not altered in the presence of a MRP2 inhibitor. Finally, biliary and canalicular clearances of atovaquone were studied in P-gp, Bcrp, Mrp2, and Bsep knockout rats. As expected, biliary concentrations of atovaquone were orders of magnitude higher relative to unbound blood concentrations in wild-type rats (Fig. 6). A typical drug undergoing biliary excretion by these bile canalicular transporters would exhibit a higher systemic AUC and liver  $K_p$ , whereas the biliary clearance would decrease considerably in transporter knockout rats relative to wild-type controls (Zamek-Gliszczynski et al., 2005; Zamek-Gliszczynski et al., 2006; Zamek-Gliszczynski et al., 2011; Zamek-Gliszczynski et al., 2012). However, the biliary clearance of atovaquone was not decreased, while systemic AUC and liver  $K_p$  were not increased, in P-gp, Bcrp Mrp2 and Bsep knockout relative to wild-type rats (Table 2), thereby ruling out the involvement of these efflux transporters in the biliary excretion of atovaquone. Collectively, these data rule out P-gp, BCRP, MRP2 and BSEP as mechanisms of atovaquone biliary excretion. Interestingly, due to reason(s) not currently understood, the canalicular clearance of atovaquone in Mrp2 and Bsep knockout rats was about 2-fold higher relative to wild-type rats. This data suggests that bile canalicular transporter(s) involved in the biliary excretion of atovaquone might be upregulated during Mrp2 or Bsep deficiency.

JPET #247254

Since mechanism(s) of atovaquone biliary excretion were not identified, rat and human SCH were used to attempt an IVIVE for biliary and canalicular clearance with an aim of investigating transport mechanism(s) involved in the biliary excretion of atovaquone. SCH have been widely employed to predict *in vivo* biliary clearance of a wide range of compounds since they express both hepatic uptake as well as bile canalicular transporters, and biliary clearance predicted with this system correlates with that observed *in vivo* in rats and humans (Abe et al., 2008). Nevertheless, the biliary clearance of atovaquone predicted using both rat and human SCH did not agree with that observed *in vivo*. Moreover, canalicular clearance, a parameter proposed to be well predicted by SCH (Nakakariya et al., 2012), was also over predicted. Collectively, these data indicate that rat and human SCH do not predict biliary clearance of atovaquone, which again highlights the unusual biliary clearance properties of atovaquone.

In summary, current studies rule out the involvement of OATPs, OCTs, OAT2 and NTCP in the hepatic uptake and P-gp, BCRP, MRP2 and BSEP in the biliary excretion of atovaquone, which is primarily cleared by biliary excretion of parent drug in humans, with  $\geq 10,000$ -fold drug concentration in bile. The unusual mechanistic basis behind the biliary excretion of atovaquone remains to be elucidated.

JPET #247254

### **Authorship contribution**

*Participated in research design:* Patel, Ellens, Zamek-Gliszczynski.

*Conducted experiments:* Patel, Johnson, Sychterz, Watson., Lewis.

*Contributed new reagents and analytic tools:* Patel.

*Performed data analysis:* Patel, Zamek-Gliszczynski.

*Wrote or contributed to the writing of the manuscript:* Patel, Polli, Zamek-Gliszczynski.

JPET #247254

## References

- Abe K, Bridges AS, Yue W and Brouwer KL (2008) In vitro biliary clearance of angiotensin II receptor blockers and 3-hydroxy-3-methylglutaryl-coenzyme A reductase inhibitors in sandwich-cultured rat hepatocytes: comparison with in vivo biliary clearance. *J Pharmacol Exp Ther* **326**:983-990.
- Bayliss MK, Bell JA, Jenner WN, Park GR and Wilson K (1999) Utility of hepatocytes to model species differences in the metabolism of loxidine and to predict pharmacokinetic parameters in rat, dog and man. *Xenobiotica* **29**:253-268.
- Davies B and Morris T (1993) Physiological parameters in laboratory animals and humans. *Pharm Res* **10**:1093-1095.
- Di L, Breen C, Chambers R, Eckley ST, Fricke R, Ghosh A, Harradine P, Kalvass JC, Ho S, Lee CA, Marathe P, Perkins EJ, Qian M, Tse S, Yan Z and Zamek-Gliszczynski MJ (2017) Industry Perspective on Contemporary Protein-Binding Methodologies: Considerations for Regulatory Drug-Drug Interaction and Related Guidelines on Highly Bound Drugs. *J Pharm Sci* **106**:3442-3452.
- Giacomini KM, Huang SM, Tweedie DJ, Benet LZ, Brouwer KL, Chu X, Dahlin A, Evers R, Fischer V, Hillgren KM, Hoffmaster KA, Ishikawa T, Keppler D, Kim RB, Lee CA, Niemi M, Polli JW, Sugiyama Y, Swaan PW, Ware JA, Wright SH, Yee SW, Zamek-Gliszczynski MJ and Zhang L (2010) Membrane transporters in drug development. *Nat Rev Drug Discov* **9**:215-236.
- Higgins JW, Ke AB and Zamek-Gliszczynski MJ (2014) Clinical CYP3A inhibitor alternatives to ketoconazole, clarithromycin and itraconazole, are not transported into the liver by hepatic organic anion transporting polypeptides and organic cation transporter 1. *Drug Metab Dispos* **42**:1780-1784.
- Kock K and Brouwer KL (2012) A perspective on efflux transport proteins in the liver. *Clin Pharmacol Ther* **92**:599-612.
- Kotani N, Maeda K, Watanabe T, Hiramatsu M, Gong LK, Bi YA, Takezawa T, Kusuhara H and Sugiyama Y (2011) Culture period-dependent changes in the uptake of transporter substrates in sandwich-cultured rat and human hepatocytes. *Drug Metab Dispos* **39**:1503-1510.
- Malarone® (2016) Product Information
- McKeage K and Scott L (2003) Atovaquone/proguanil: a review of its use for the prophylaxis of Plasmodium falciparum malaria. *Drugs* **63**:597-623.
- Mepron® (2016) Product Information
- Mohamed LA and Kaddoumi A (2013) In vitro investigation of amyloid-beta hepatobiliary disposition in sandwich-cultured primary rat hepatocytes. *Drug Metab Dispos* **41**:1787-1796.
- Nakakariya M, Ono M, Amano N, Moriwaki T, Maeda K and Sugiyama Y (2012) In vivo biliary clearance should be predicted by intrinsic biliary clearance in sandwich-cultured hepatocytes. *Drug Metab Dispos* **40**:602-609.
- Nixon GL, Moss DM, Shone AE, Laloo DG, Fisher N, O'Neill PM, Ward SA and Biagini GA (2013) Antimalarial pharmacology and therapeutics of atovaquone. *J Antimicrob Chemother* **68**:977-985.
- Patel M, Taskar KS and Zamek-Gliszczynski MJ (2016) Importance of Hepatic Transporters in Clinical Disposition of Drugs and Their Metabolites. *J Clin Pharmacol* **56 Suppl 7**:S23-39.
- Riley RJ, Foley SA, Barton P, Soars MG and Williamson B (2016) Hepatic drug transporters: the journey so far. *Expert Opin Drug Metab Toxicol* **12**:201-216.
- Rolan PE, Mercer AJ, Tate E, Benjamin I and Posner J (1997) Disposition of atovaquone in humans. *Antimicrob Agents Chemother* **41**:1319-1321.
- Wolf KK, Brouwer KR, Pollack GM and Brouwer KL (2008) Effect of albumin on the biliary clearance of compounds in sandwich-cultured rat hepatocytes. *Drug Metab Dispos* **36**:2086-2092.

JPET #247254

- Zamek-Gliszczyński MJ, Bedwell DW, Bao JQ and Higgins JW (2012) Characterization of SAGE Mdr1a (P-gp), Bcrp, and Mrp2 knockout rats using loperamide, paclitaxel, sulfasalazine, and carboxydichlorofluorescein pharmacokinetics. *Drug Metab Dispos* **40**:1825-1833.
- Zamek-Gliszczyński MJ, Day JS, Hillgren KM and Phillips DL (2011) Efflux transport is an important determinant of ethinylestradiol glucuronide and ethinylestradiol sulfate pharmacokinetics. *Drug Metab Dispos* **39**:1794-1800.
- Zamek-Gliszczyński MJ, Hoffmaster KA, Humphreys JE, Tian X, Nezasa K and Brouwer KL (2006) Differential involvement of Mrp2 (Abcc2) and Bcrp (Abcg2) in biliary excretion of 4-methylumbelliferyl glucuronide and sulfate in the rat. *J Pharmacol Exp Ther* **319**:459-467.
- Zamek-Gliszczyński MJ, Hoffmaster KA, Tian X, Zhao R, Polli JW, Humphreys JE, Webster LO, Bridges AS, Kalvass JC and Brouwer KL (2005) Multiple mechanisms are involved in the biliary excretion of acetaminophen sulfate in the rat: role of Mrp2 and Bcrp1. *Drug Metab Dispos* **33**:1158-1165.

JPET #247254

## Figure Legends

Fig. 1: Structure of atovaquone.

Fig. 2: The ratio of the uptake of A) [<sup>3</sup>H]-Estradiol 17β-D-glucuronide (EG) in HEK-OATP1B1 relative to control cells in the absence or presence of 10 μM rifamycin for 5 min, B) [<sup>3</sup>H]-EG in HEK-OATP1B3 and control cells in the absence or presence of 10 μM rifamycin for 10 min, C) [<sup>3</sup>H]-Estrone Sulfate (ES) in HEK-OATP2B1 and control cells in the absence or presence of 30 μM montelukast for 5 min, D) [<sup>14</sup>C]-Metformin hydrochloride (MF) in HEK-OCT1 and control cells in the absence or presence of 100 μM imipramine for 15 min, E) [<sup>3</sup>H]-Cyclic guanosine monophosphate (cGMP) in HEK-OAT2 and control cells in the absence or presence of 100 μM indomethacin for 2 min and F) [<sup>3</sup>H]-Taurocholic acid (TCA) in HEK-NTCP and control cells in the absence or presence of 10 μM cyclosporine for 5 min. Uptake of atovaquone (ATQ, 1.5 μM) was carried out simultaneously with positive controls in singly expressing and control cells in the absence or presence of transporter inhibitors at 37°C for 1 and 10 min, respectively. Unfilled bar represents the ratio of uptake in singly expressing to control cells in the absence of inhibitors. Filled bars represents the ratio of uptake in singly expressing to control cells in the presence of transporter inhibitors. Mean ± standard deviation, n=4, \**p* < 0.05.

Fig. 3: Uptake clearance of [<sup>3</sup>H]-Estradiol 17β-D-glucuronide (EG, 0.02 μM) and atovaquone (ATQ, 2.5 μM) in the absence or presence of an OATP and OCT inhibitor cocktail (rifamycin and imipramine, 100 μM each) in cryopreserved pooled plated human hepatocytes. Mean ± standard deviation, n=3, \**p* < 0.05.

JPET #247254

Fig. 4: Atovaquone blood concentration versus time profile following a single IV bolus dose of 1 mg/kg to Oatp1a/1b knockout (▲), Oct1/2 knockout (◆) and FVB wild-type (○) mice. Mean ± standard deviation, n=4.

Fig. 5: A) Efflux ratio of [<sup>3</sup>H]-Amprenavir (APV) and atovaquone (ATQ, 2.5 μM) in the absence or presence of GF120918 across MDCK-MDR1 cell monolayer. B) Efflux ratio of [<sup>14</sup>C]-Cimetidine (CIM) and ATQ (2.5 μM) in the absence or presence of GF120918 across MDCK-BCRP cell monolayer. C) Uptake rate of [<sup>3</sup>H]-Estradiol 17β-D-glucuronide (EG) and atovaquone (ATQ, 2.5 μM) in the presence of ATP or AMP as well as in the presence of bromosulphophthalein (BSP) and ATP in MRP2 vesicles. Mean ± standard deviation, n=3, \**p* < 0.05.

Fig. 6: Atovaquone unbound blood (○) and bile (●) concentration versus time profile following an IV bolus dose of 2.5 mg/kg and continuous infusion at 0.1 mg/h/kg in wild-type male Sprague Dawley rats. Mean ± standard deviation, n=4.

JPET #247254

## Tables

**Table 1:** Pharmacokinetic parameters of atovaquone following a single IV bolus dose of 1 mg/kg in Oatp1a/1b knockout, Oct1/2 knockout and wild-type FVB mice. Mean  $\pm$  standard deviation, n=4.

Parameters	Wild Type FVB	Oatp1a/1b Knockout	Oct1/2 Knockout
AUC <sub>(0-30)</sub> ( $\mu\text{g}\cdot\text{h}/\text{mL}$ )	24 $\pm$ 3	18 $\pm$ 1	29.5 $\pm$ 0.4
CL <sub>obs</sub> (mL/min/kg)	0.53 $\pm$ 0.05	0.86 $\pm$ 0.07	0.46 $\pm$ 0.05
V <sub>ss</sub> (L/kg)	0.7 $\pm$ 0.1	0.7 $\pm$ 0.1	0.50 $\pm$ 0.08
Liver K <sub>p</sub>	0.49 $\pm$ 0.06	0.61 $\pm$ 0.11	0.53 $\pm$ 0.06

Note: Liver K<sub>p</sub> values were calculated as the ratio of atovaquone liver to blood concentrations at distributional equilibrium (30 h).

JPET #247254

**Table 2:** Pharmacokinetic parameters of atovaquone following a loading IV bolus dose of 2.5 mg/kg followed by a continuous infusion of 0.1 mg/kg/h in P-gp, Bcrp, Mrp2, Bsep knockout and wild-type male Sprague-Dawley rats.

Pharmacokinetic parameters	Wild Type	P-gp Knockout	Bcrp Knockout	Mrp2 Knockout	Bsep Knockout
AUC <sub>(0-30)</sub> (μmol.h/mL)	0.45 ± 0.05	0.44 ± 0.05	0.44 ± 0.01	0.34 ± 0.06	0.46 ± 0.06
Bile recovery (nmol)	235 ± 61	241 ± 33	194 ± 32	301 ± 108	340 ± 46
S.S. biliary excretion rate (nmol/h)	6.9 ± 1.2	7.0 ± 0.7	5.2 ± 0.9	9 ± 4	9.6 ± 1.7
S.S. liver Conc. (μM)	5.3 ± 0.7	5.4 ± 0.7	5.1 ± 0.8	4.3 ± 0.6	4.5 ± 0.7
S.S. Liver K <sub>p</sub>	0.36 ± 0.05	0.38 ± 0.04	0.35 ± 0.06	0.40 ± 0.08	0.32 ± 0.02
S.S. biliary clearance (mL/min/kg)	0.029 ± 0.007	0.029 ± 0.005	0.024 ± 0.003	0.06 ± 0.02	0.04 ± 0.01
S.S. canalicular clearance (mL/min/kg)	0.07 ± 0.01	0.07 ± 0.02	0.06 ± 0.01	0.14 ± 0.03*	0.12 ± 0.04

Note: S.S. represents steady-state. Biliary excretion rate was calculated as an average from 4-30 h in all rat groups. Liver K<sub>p</sub> was calculated as a ratio of atovaquone liver to blood concentration at 30 h. Mean ± standard deviation, n=4-6, \**p* < 0.05.

JPET #247254

**Table 3:** Predicted biliary and canalicular clearances of atovaquone using rat and human SCH.

Parameters	Rat SCH	Human SCH
Predicted biliary clearance (Eq. 6)	$19 \pm 15$	$2.2 \pm 2.4$
Predicted biliary clearance (Eq. 7)	$0.04 \pm 0.04$	$0.003 \pm 0.003$
Predicted canalicular clearance (Eq. 8, 9)	$0.8 \pm 0.6$	ND

Note: Predicted clearances are expressed as mL/min/kg. ND: Not determined.

JPET #247254

## Figures

**Fig. 1**

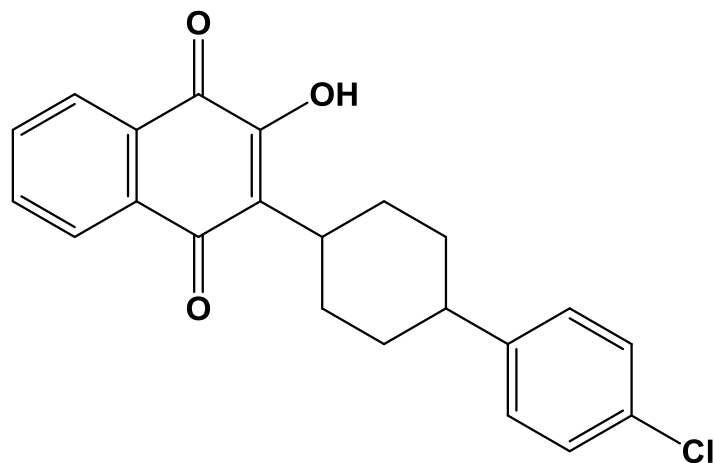
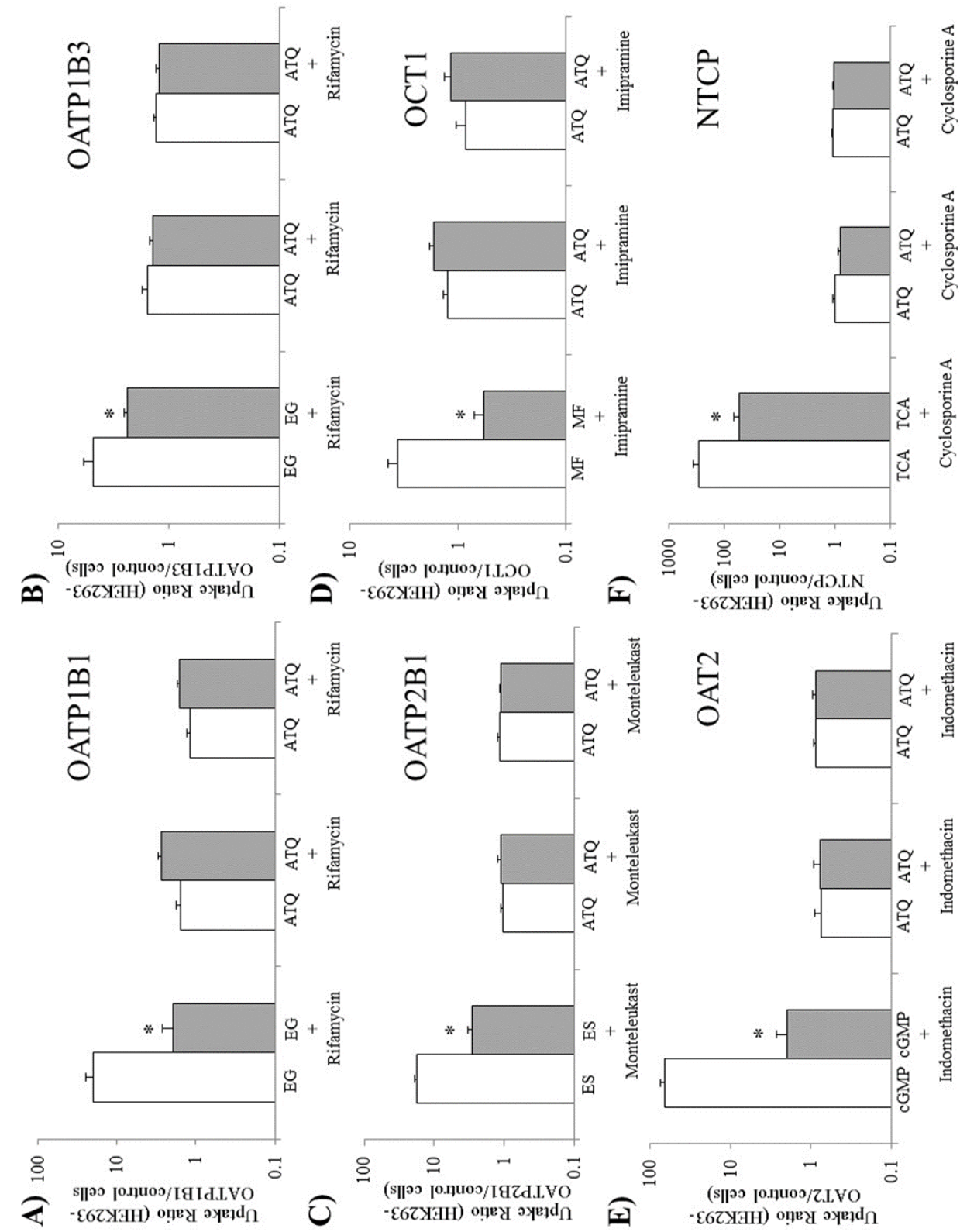
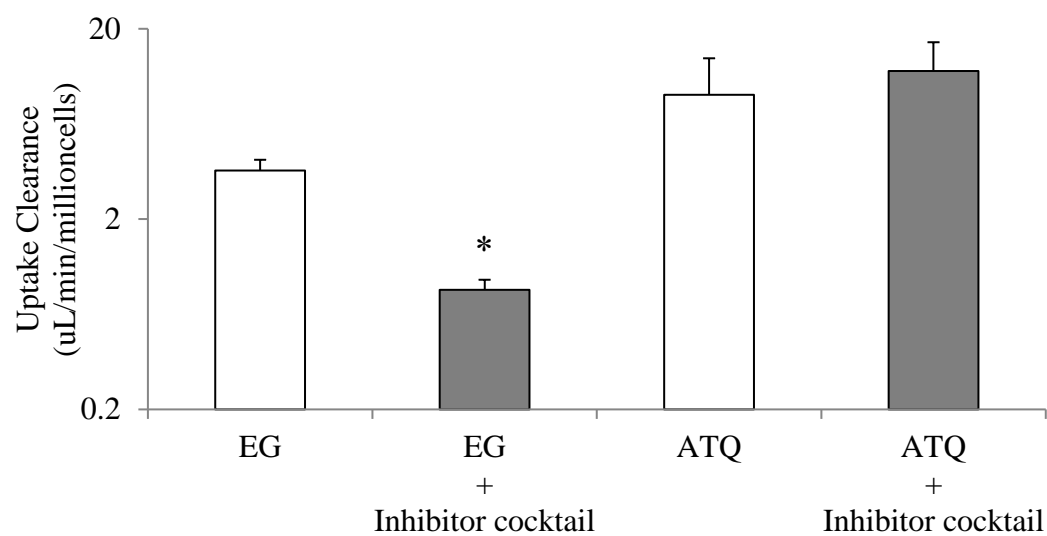


Fig. 2



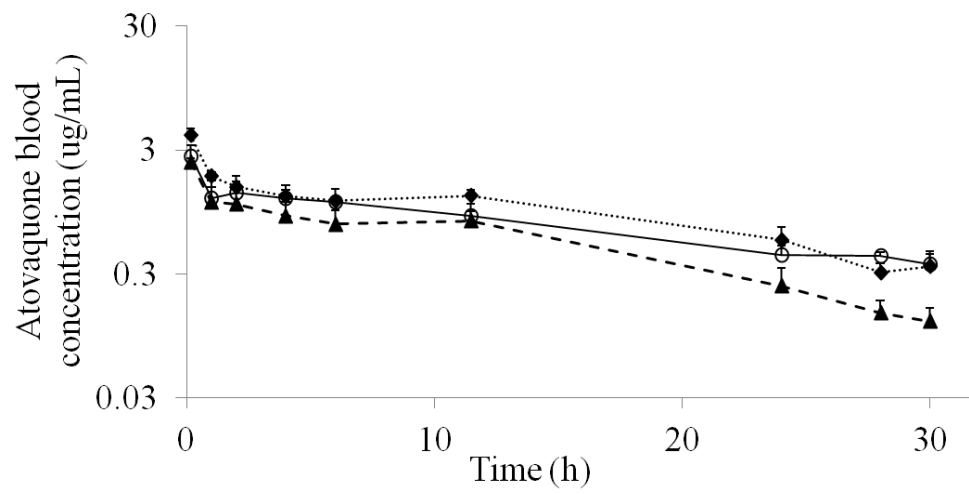
JPET #247254

**Fig. 3**



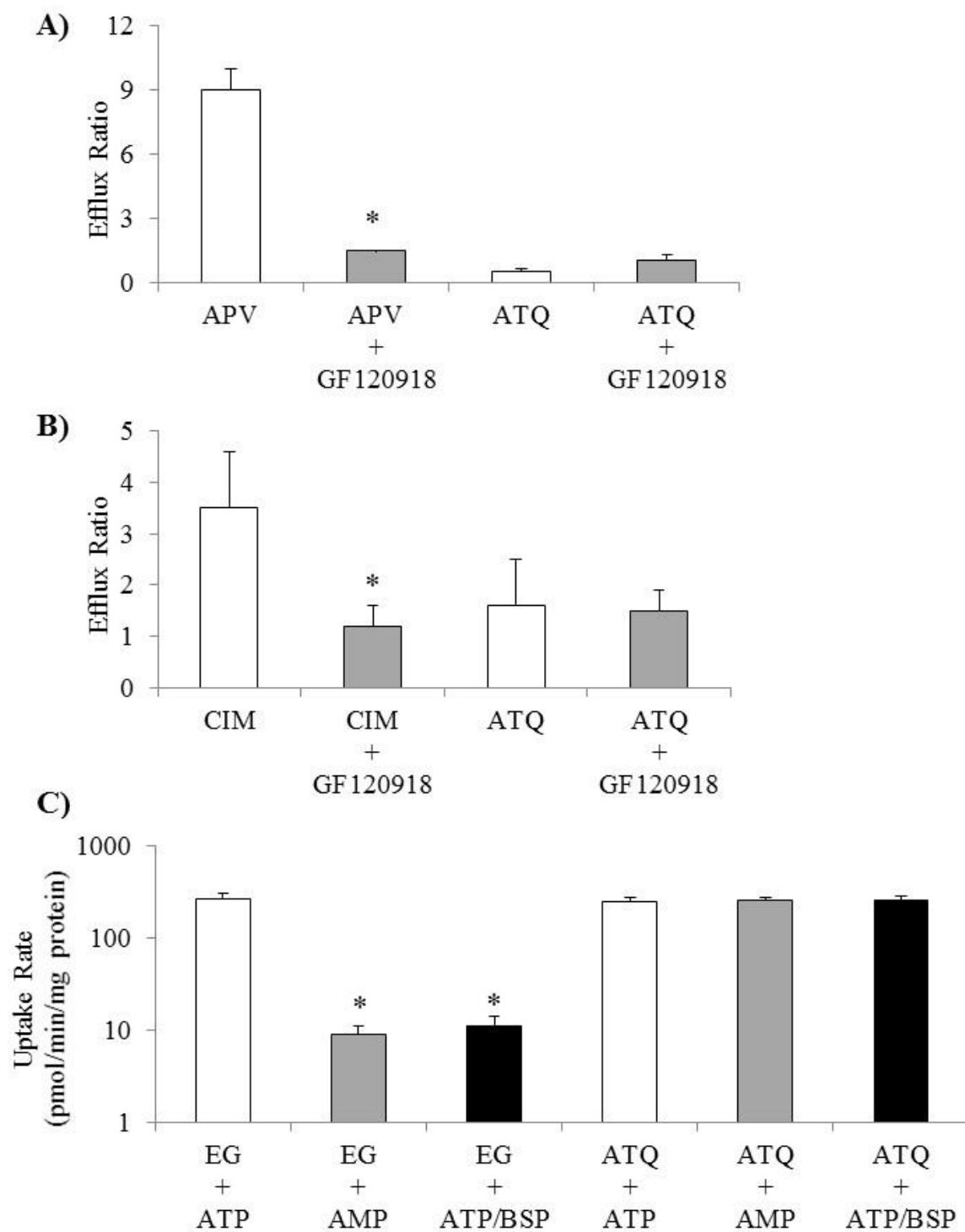
JPET #247254

**Fig. 4**



JPET #247254

**Fig. 5**



JPET #247254

**Fig. 6**

